

High-performance vertical polymer nanorod transistors based on air-stable conjugated polymer

Yu-Chiang Chao, Chin-Ho Chung, Hsiao-Wen Zan, Hsin-Fei Meng, and Ming-Che Ku

Citation: *Applied Physics Letters* **99**, 233308 (2011); doi: 10.1063/1.3668086

View online: <http://dx.doi.org/10.1063/1.3668086>

View Table of Contents: <http://scitation.aip.org/content/aip/journal/apl/99/23?ver=pdfcov>

Published by the [AIP Publishing](#)

Articles you may be interested in

[High-performance, low-operating voltage, and solution-processable organic field-effect transistor with silk fibroin as the gate dielectric](#)

Appl. Phys. Lett. **104**, 023302 (2014); 10.1063/1.4862198

[Operational stability enhancement of low-voltage organic field-effect transistors based on bilayer polymer dielectrics](#)

Appl. Phys. Lett. **103**, 133303 (2013); 10.1063/1.4822181

[Air-stable -conjugated amorphous copolymer field-effect transistors with high mobility of 0.3cm²/Vs](#)

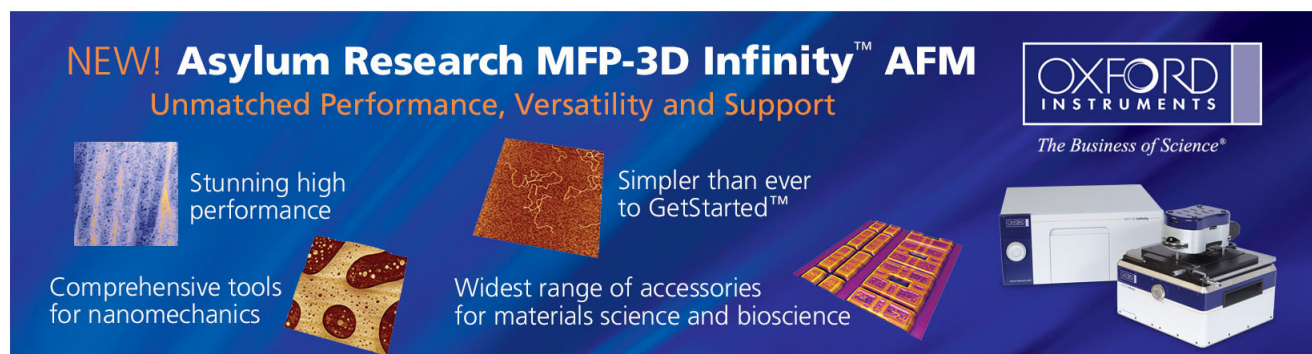
Appl. Phys. Lett. **101**, 213305 (2012); 10.1063/1.4767921

[High output current in vertical polymer space-charge-limited transistor induced by self-assembled monolayer](#)

Appl. Phys. Lett. **101**, 093307 (2012); 10.1063/1.4748284

[High-performance organic integrated circuits based on solution processable polymer-small molecule blends](#)

Appl. Phys. Lett. **93**, 253301 (2008); 10.1063/1.3050525

The advertisement features a dark blue background with white and orange text. At the top left, it reads 'NEW! Asylum Research MFP-3D Infinity™ AFM' in large white letters, followed by 'Unmatched Performance, Versatility and Support' in orange. The Oxford Instruments logo is in the top right, with the tagline 'The Business of Science®'. Below the text are four images: a blue textured surface, a brown textured surface, a yellow and red patterned surface, and a photograph of the AFM instrument. Each image is accompanied by a short text description: 'Stunning high performance', 'Simpler than ever to GetStarted™', 'Comprehensive tools for nanomechanics', and 'Widest range of accessories for materials science and bioscience'.

High-performance vertical polymer nanorod transistors based on air-stable conjugated polymer

Yu-Chiang Chao,¹ Chin-Ho Chung,¹ Hsiao-Wen Zan,^{2,a)} Hsin-Fei Meng,^{1,a)} and Ming-Che Ku²

¹*Institute of Physics, National Chiao Tung University, HsinChu 300, Taiwan*

²*Department of Photonics and Institute of Electro-Optical Engineering, National Chiao Tung University, HsinChu 300, Taiwan*

(Received 23 September 2011; accepted 18 November 2011; published online 9 December 2011)

A vertical polymer nanorod transistor was realized based on an air-stable poly[5,5'-bis(3-dodecyl-2-thienyl)-2,2'-bithiophene] with a high highest occupied molecular orbital energy level. The influence of the work function of the emitter on the performances of the space-charge-limited transistor was investigated. When MoO₃/Al was used as the top emitter and indium tin oxide was used as the bottom collector, the operating voltage of 0.6 V, the on/off current ratio of 4×10^4 , and the switching swing of 105 mV/decade were achieved. A low-power-consumption inverter was also demonstrated. © 2011 American Institute of Physics. [doi:10.1063/1.3668086]

Organic nanostructures, such as nanowires and nanorods, with self-assembled molecular stacking have attracted significant attention in the past few years.¹ Highly organized molecules induce a strong overlap between electronic wave functions of neighboring molecules, leading to high carrier mobilities.² Nanostructures of conjugated small molecules or polymers have been demonstrated to be promising for both organic solar cells^{3,4} and organic field-effect transistors (OFETs).^{5–7} The poly(3-hexylthiophene) (P3HT) nanorods oriented perpendicularly to the substrate, which can be fabricated by using block copolymer⁸ and anodized aluminum oxide^{9,10} as templates, have been used as donor material in organic solar cells.⁹ The performances of the organic solar cells that incorporate polymer nanorods were enhanced because the chain alignment and the carrier mobility in the nanorods were improved.^{9–11} Another device that incorporates the polymer nanorods is the polymer vertical transistor, named as the polymer space-charge-limited transistor (SCLT),^{12–15} which has a vertical channel length (*L*) of a few hundred nanometers. The chain alignment and the carrier mobility of the P3HT have been demonstrated to be enhanced by the cylindrical nanopores with a slow solvent annealing process.¹⁴ In the active area of the conventional SCLT, the holes are injected into the semiconducting polymer nanorods by the emitter at the bottom of the SCLT, passing through the openings on the base, and being collected by the collector. The voltages applied at the base and the collector control the magnitude of the potential barrier inside the carrier channel and hence the on and off states of the SCLT. In our previous report, an Al top electrode was used as the collector, and the indium tin oxide (ITO) bottom electrode was used as the emitter.^{12–15} The oxygen plasma treatment was required to enhance the work function of the ITO emitter for a better carrier injection property.¹² However, the work function of the oxygen plasma-treated ITO was unstable.¹² In addition, P3HT is not an air-stable semiconducting poly-

mer, which shows degradation of electrical characteristics in ambient.¹⁶ Semiconducting polymers such as poly[5,5'-bis(3-dodecyl-2-thienyl)-2,2'-bithiophene] (PQT-12)¹⁷ and poly(2,5-bis(3-tetradecylthiophen-2-yl)thieno[3,2-b]thiophene) (PBTTT)¹⁸ were, therefore, synthesized with better air stability and carrier mobility than that of the P3HT. However, since the highest occupied molecular orbital (HOMO) levels of PQT-12 and PBTTT (HOMO_{PQT-12} = -5.24 eV, HOMO_{PBTTT} = -5.10 eV)^{19,20} are higher than the work function of the oxygen plasma-treated ITO, the carrier injection barrier is large which hinders the application of the PQT-12 and the PBTTT for conventional SCLT using bottom ITO as the emitter.

In this work, an SCLT structure suitable for air-stable conjugated polymer is realized by using the high work function MoO₃/Al as the top emitter and the ITO as the bottom collector. The air-stable conjugated polymer PQT-12 was used as the active material. The operating voltage is 0.6 V, the on/off current ratio is 4×10^4 , and the switching swing is 105 mV/decade. An inverter fabricated by connecting a PQT-12 SCLT with a resistor in series is also demonstrated.

The schematic device structure is shown in Fig. 1(a). Devices were prepared on ITO glass substrates treated by 150 W O₂ plasma (RF) for 30 min. A layer of 200 nm cross-linked poly(4-vinyl phenol) (PVP) was prepared by spin-coating a blend solution of PVP and methylated poly(melamineco-formaldehyde) on the ITO substrate and then cross-linking at 200 °C for 1 h. A layer of P3HT (Rieke Metal) was spin coated on PVP, annealed at 200 °C for 10 min, and spin rinsed by xylene to form a thin layer of 15 nm. The polystyrene (PS) spheres of 100 nm diameter were adsorbed on the P3HT surface as the shadow masks by submerging the substrate into a dilute ethanol solution (0.4%) of negatively charged PS spheres (Fluka) for 1 min. After transferring the substrate to a beaker of boiling isopropanol solution for 10 s, the substrate was blow dried immediately, and a non-close-packed PS spheres array was formed. Al of 60 nm was deposited as the base electrode, and then the PS spheres were removed by adhesive tape (Scotch,

^{a)}Authors to whom correspondence should be addressed. Electronic addresses: hsiaowen@mail.nctu.edu.tw and meng@mail.nctu.edu.tw.

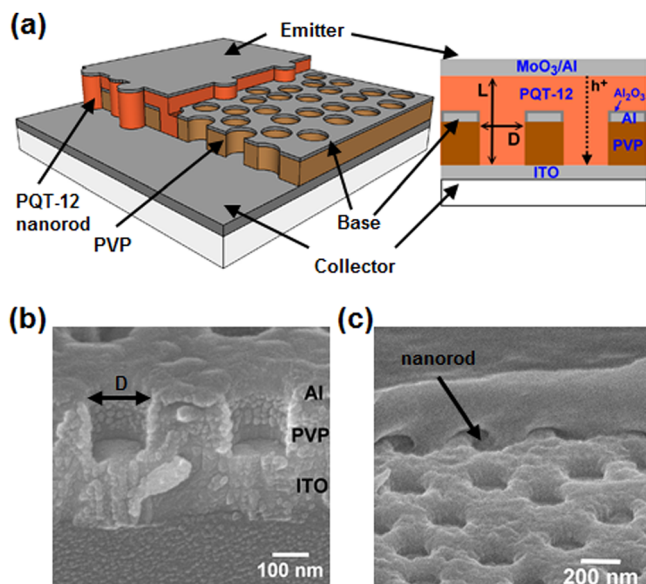


FIG. 1. (Color online) (a) Schematic device structure of SCLT. The opening diameter is denoted by D , and the channel length is denoted by L . (b) The scanning electron microscope image of the vertically oriented PVP cylindrical nanopores with base on top. (c) The scanning electron microscope image of the device after coating semiconducting polymer. Partial semiconducting polymer is tore off to unveil polymer nanorods. The polymer nanorods can be seen in the vertically oriented PVP cylindrical nanopores with some distortion, which was caused when tearing off polymer.

3 M). The PVP at the sites without Al coverage was removed by 150 W O_2 plasma (RF), and the vertically oriented PVP cylindrical nanopores were formed as shown in Fig. 1(b). The diameters of the opening diameter (D) and the vertically oriented cylindrical nanopores are, therefore, equal to the diameter of the PS sphere. 350 nm of P3HT or PQT-12 (American Dye Source) in chlorobenzene was coated as the active material, and then the polymer forms nanorods inside the vertically oriented PVP cylindrical nanopores as shown in Fig. 1(c). Finally, MoO_3 (10 nm)/Al (40 nm) was deposited to complete the SCLT with an active area of 1 mm^2 . The formula $[\delta(\log J_C)/\delta(V_{BE})]^{-1}$ was used to extract the switching swings of the SCLTs from the transfer characteristics when the collector to emitter voltage (V_{CE}) was fixed. J_C and V_{BE} are the output current density and the base-to-emitter voltage of the SCLT. We use the term switching swing for SCLTs, because the operation principles of the SCLTs and the OFETs are different.

The diodes of P3HT and PQT-12 with different electrodes were prepared as a first step to understand the influence of the work function of the electrodes on hole injection properties. The current density (J)–electric field (E) curves of these diodes are shown in Fig. 2(a). The work functions of electrodes as well as the HOMO and the lowest unoccupied molecular orbital (LUMO) levels of the P3HT and the PQT-12 are shown in Fig. 2(b). The molecular structures of the P3HT and the PQT-12 are shown in Fig. 2(c). When the ITO bottom electrode is positively biased, the holes are able to be injected to the P3HT from the oxygen plasma-treated ITO since the work function of oxygen plasma-treated ITO is about 5 eV which makes the hole injection barrier between oxygen plasma-treated ITO and P3HT negligible.¹² However, since there is a hole injection barrier between the oxy-

gen plasma-treated ITO and the PQT-12, it is much more difficult for the holes to be injected into the PQT-12, and hence, the current density is low. On the other hand, when negative bias is applied to the ITO bottom electrode, holes are injected from top electrode. The current densities of both the P3HT and the PQT-12 diodes with MoO_3/Al top electrodes are larger than the diodes with Al top electrodes. This is attributed to the higher work function of the MoO_3/Al which makes the MoO_3/Al a better hole injection electrode than the Al and the oxygen plasma-treated ITO. An SCLT suitable for air-stable PQT-12 could be developed by using MoO_3/Al as top emitter.

The transfer and output characteristics of the PQT-12 SCLT and P3HT SCLT using MoO_3/Al as top emitter and ITO as bottom collector were investigated and shown in Fig. 3. The D and L are 100 nm and 350 nm, respectively. The transistor characteristics of the bottom and the top injection P3HT SCLTs are similar. The switching swing is about 135 mV/decade, and the on/off current ratio is about 2×10^4 . However, no transistor characteristics can be observed for the bottom injection PQT-12 SCLTs, because the ITO bottom electrode is not a good hole injection electrode for PQT-12. For top injection PQT-12 SCLTs, normal transistor characteristics can be obtained. This is because the MoO_3/Al is a good hole injection electrode for PQT-12. The operation voltage is only 0.6 V. The switching swing of 105 mV/decade and the on/off current ratio of 4×10^4 are obtained. Such

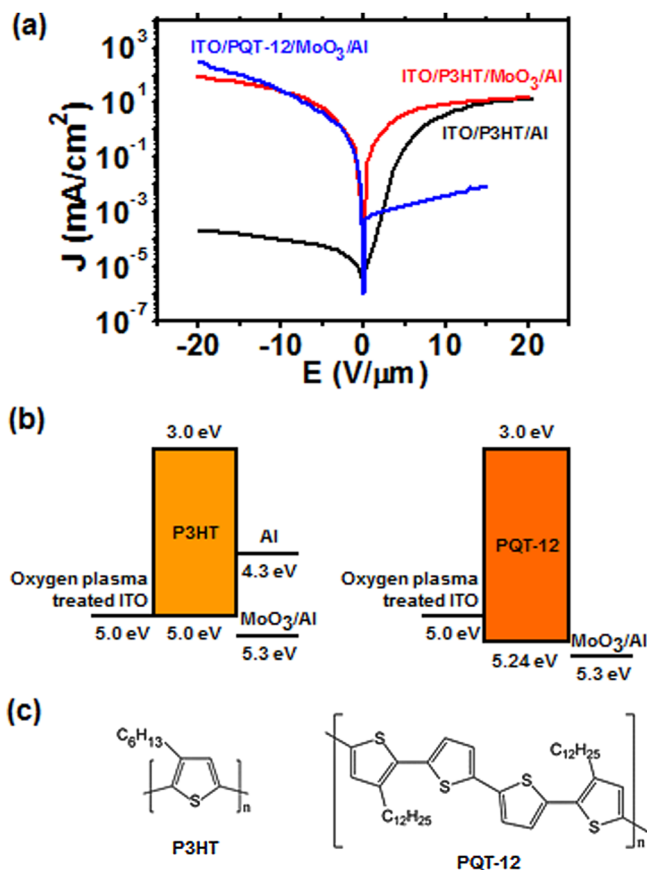


FIG. 2. (Color online) (a) The current density (J)–electric field (E) curves of P3HT and PQT-12 diodes. (b) The electrode work functions as well as HOMO and LUMO levels of P3HT and PQT-12. (c) Molecular structures of P3HT and PQT-12.

a low operation voltage and a low switching swing are superior to those of OFETs. This is the first time, without compromising transistor performances, that an air-stable semiconducting polymer with a high HOMO energy level is used as the active material for SCLT. Other high-performance semiconducting polymers with similar or lower HOMO energy levels could also be used as the active material for this SCLT structure.

A resistive-load inverter based on PQT-12 SCLT was then realized by connecting a top injection PQT-12 SCLT with a load resistor (R_L) in series to demonstrate the PQT-12 SCLT's application in logic circuit. The schematic inverter circuit is shown in the inset of Fig. 4(a). The transfer characteristics of the inverter at various R_L are shown in Fig. 4(a). The supply voltage (V_{DD}) is fixed at -1.8 V while the input voltage (V_{in}) is varied from -0.8 to 0.4 V. When the V_{in} is 0.4 V, the PQT-12 SCLT is in the off state with a high effective resistance, and the output voltage (V_{out}) approaches V_{DD} . When the V_{in} is -0.8 V, the PQT-12 SCLT is in the on state with a low effective resistance, and the V_{out} approaches 0 V. As shown in Fig. 4(b), when $R_L = 20$ M Ω , the absolute value of the voltage gain is 9.35 which is the highest value of various vertical transistors. This demonstrates that the PQT-12 can be used in low-operation-voltage and low-power-consumption electronic devices.

In summary, a vertical polymer nanorod transistor was realized for air-stable semiconducting polymer with a high HOMO energy level. High work function electrode was used

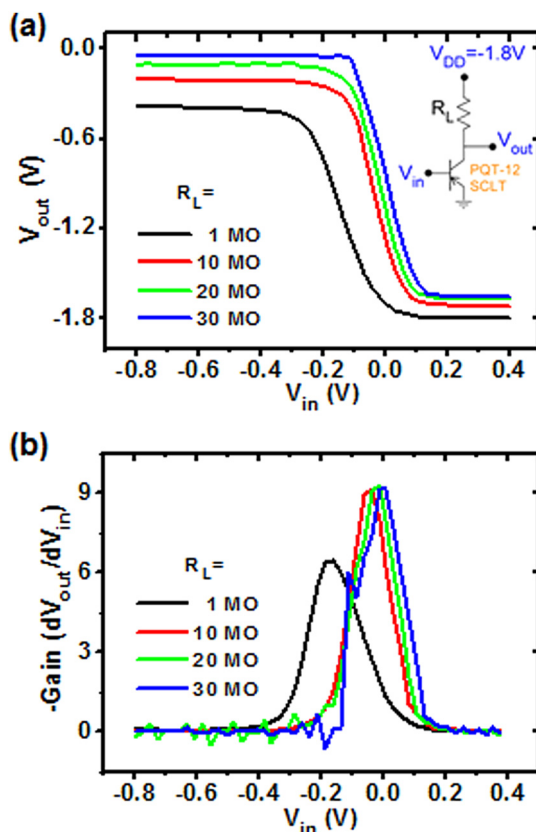


FIG. 4. (Color online) (a) The transfer characteristics and (b) the voltage gain of the inverter. The inset shows the schematic inverter circuit.

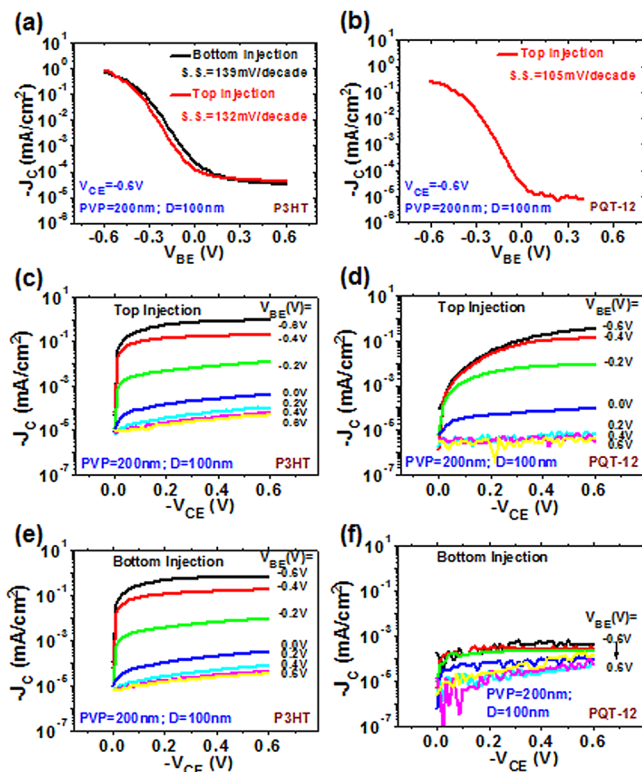


FIG. 3. (Color online) The transfer characteristics of the bottom and the top injection SCLTs with $D = 100$ nm made by (a) P3HT and (b) PQT-12. The output characteristics of the top injection SCLTs with $D = 100$ nm made by (c) P3HT and (d) PQT-12. The output characteristics of the bottom injection SCLTs with $D = 100$ nm made by (e) P3HT and (f) PQT-12. The thickness of PVP and the channel length L are fixed at 200 nm and 350 nm, respectively.

for better hole injection. The operating voltage of 0.6 V, the on/off current ratio of 4×10^4 , and the switching swing of 105 mV/decade were obtained. A low-voltage inverter was demonstrated which fulfills the requirement of the low-power-consumption logic circuit.

This work was supported by the National Science Council of Taiwan under Contract No. NSC100-2628-M-009-002-.

- ¹A. L. Briseno, S. C. B. Mannsfeld, S. A. Jenekhe, Z. Bao, and Y. Xia, *Mater. Today* **11**, 38 (2008).
- ²M. D. Curtis, J. Cao, and J. W. Kampf, *J. Am. Chem. Soc.* **126**, 4318 (2004).
- ³R. J. Tseng, R. Chan, V. C. Tung, and Y. Yang, *Adv. Mater.* **20**, 435 (2008).
- ⁴S. Berson, R. D. Bettignies, S. Bailly, and S. Guillerez, *Adv. Funct. Mater.* **17**, 1377 (2007).
- ⁵J. P. Hong, M. C. Um, S. R. Nam, J. I. Hong, and S. Lee, *Chem. Commun.* **310** (2009).
- ⁶A. L. Briseno, S. C. B. Mannsfeld, M. M. Ling, S. Liu, R. J. Tseng, C. Reese, M. E. Roberts, Y. Yang, F. Wudl, and Z. Bao, *Nature* **444**, 913 (2006).
- ⁷D. H. Kim, J. T. Han, Y. D. Park, Y. Jang, J. H. Cho, M. Hwang, and K. Cho, *Adv. Mater.* **18**, 719 (2006).
- ⁸J. I. Lee, S. H. Cho, S. M. Park, J. K. Kim, J. K. Kim, J. W. Yu, Y. C. Kim, and T. P. Russell, *Nano Lett.* **8**, 2315 (2008).
- ⁹J. S. Kim, Y. Park, D. Y. Lee, J. H. Lee, J. H. Park, J. K. Kim, and K. Cho, *Adv. Funct. Mater.* **20**, 540 (2010).
- ¹⁰K. M. Coakley, B. S. Srinivasan, J. M. Ziebarth, C. Goh, Y. Liu, and M. D. McGehee, *Adv. Funct. Mater.* **15**, 1927 (2005).
- ¹¹M. Aryal, K. Trivedi, and W. Hu, *ACS Nano* **3**, 3085 (2009).
- ¹²Y. C. Chao, Y. C. Lin, M. Z. Dai, H. W. Zan, and H. F. Meng, *Appl. Phys. Lett.* **95**, 203305 (2009).
- ¹³Y. C. Chao, M. C. Ku, W. W. Tsai, H. W. Zan, H. F. Meng, and H. K. Tsai, *Appl. Phys. Lett.* **97**, 223307 (2010).
- ¹⁴Y. C. Chao, M. C. Niu, H. W. Zan, H. F. Meng, and M. C. Ku, *Org. Electron.* **12**, 78 (2011).

- ¹⁵Y. C. Chao, C. Y. Chen, H. W. Zan, and H. F. Meng, *J. Phys. D: Appl. Phys.* **43**, 205101 (2010).
- ¹⁶S. Hoshino, M. Yoshida, S. Uemura, T. Kodzasa, N. Takada, T. Kamata, and K. Yase, *J. Appl. Phys.* **95**, 5088 (2004).
- ¹⁷B. S. Ong, Y. Wu, P. Liu, and S. Gardner, *J. Am. Chem. Soc.* **126**, 3378 (2004).
- ¹⁸S. Wang, J. C. Tang, L. H. Zhao, R. Q. Png, L. Y. Wong, P. J. Chia, H. S. O. Chan, P. K.-H. Ho, and L. L. Chua, *Appl. Phys. Lett.* **92**, 162103 (2008).
- ¹⁹B. S. Ong, Y. Wu, P. Liu, and S. Gardner, *Adv. Mater.* **17**, 1141 (2005).
- ²⁰J. E. Parmer, A. C. Mayer, B. E. Hardin, S. R. Scully, M. D. McGehee, M. Heeney, and I. McCulloch, *Appl. Phys. Lett.* **92**, 113309 (2008).